

Effect of vertical load on tailings particles

Juan Manuel Rodriguez¹, Riaz Bhanbhro² Tommy Edeskär³ and Sven Knutsson⁴

Abstract

Tailing dams could store hundreds, thousands or millions of cubic meters of tailings result of the mining extractive industry. Mechanical behavior of this man-made soil should be known in order to maintain a safe storage. Dykes rise up to form the dams and they are buildup with the same tailing material especially in the upstream method using the coarse part. The study uses oedometer classical test to determine the load effect over tailing coarse particles. Tailings are site specific and so its characteristics. It is necessary to understand the tailings degradations to achieve safe impounds. The study comprises four samples of one range-size tailing particles (e.g. 1-0.5, 0.5-0.25, 0.25-0.125, 0.125-0.063mm) subject to vertical load in traditional oedometers. Vertical load effects are measured using two dimensional image analysis and sieving. Results show that 0.063mm sample is the only one that has change in shape with low breakage (<1%) while the rest of the sizes have no shape change but high breakage is present especially in fraction 0.5mm. Settlements also are more pronounced in coarse fractions 0.5 and 0.25mm.

Keywords: Tailings, Compression, Degradation, Deformation

1 Introduction

Tailings are the waste from ore concentration in the mining industry and they are usually deposited in tailings dams. Tailings dams are typically huge constructions

¹Luleå University of Technology. e-mail: juan.rodriguez@ltu.se

²Luleå University of Technology. e-mail: riaz.bahnbhro@ltu.se

³Luleå University of Technology. e-mail: tommy.edeskar@ltu.se

⁴Luleå University of Technology. e-mail: sven.knutsson@ltu.se

and can cover a surface of a couple of square kilometers and be raised to hundred meters high [1]. Storage facilities for tailings need to be safe, structurally and environmentally, in long time perspective. Tailing are the product of mechanical fracturing (crushing and milling) and site specific, as a result they are in general considered to be angular in the range from silt to fine sand [2,3]. Garga et al. [4]classifies the shape of tailings in the range from angular to sub angular.

The most economical method to upraise tailing dams is the so called upstream method. The upstream method consists in the use of the coarse part of the tailings to rise up dykes. The discharge of tailings slurry (spigots or cyclones) develops a dike and a beach composed of coarse material (not well graded). Fines and slimes are drag by the flowing water away from the dyke and beach (into the pool). The beach becomes the foundation for the next dyke [5].

According to Harding [6] the degree of which particle breakage occurs during load and deformation affects the strength and stress-strain behavior of the elements. Tailing particles under tenths of meters of material (after a couple of dykes) subject to loads and deformations could break and change strength and stress-strain behavior. Crushing of the particles under stress (under meters of soil e.g. inside the initials tailing dam dykes) depend on factors as particle size distribution, particle shape, void ratio, particle hardness (of all its components), water presence, state of the effective stress, effective stress path [6] and number of contacts per particle [7].

Breakage of the tailing particles into dykes could head for new configuration in the material, e.g. size distribution [8] or particle shape that would change properties as void ratio [9], shear strength [10], permeability (clogging particle skeleton), etc.

The scope of the study is to determine the degradation effects of tailings subject to one-dimensional load using classical oedometer test, sieving and, shape changes using image analysis software. It is accomplished by comparing results from four particle size ranges. Eleven shape descriptors are included. Results show that for all specimens except the smallest particle size, particles breakage produces a relative high amount of fines with no change of shape. Additionally for the smallest particle size sample low breakage and shape change is recognized. By comparing natural geological materials with tailings the settlements seems to be determined by the initial void ratio higher in coarse materials but also in tailings.

2 Methodology

In this study samples from the Aitik mine has been used. The Aitik tailing dam is located about 100 km North of the Arctic Circle in the boreal parts of Northern Sweden (Figure 1) about 15 km from the community of Gällivare. The value mineral is chalcopyrite (CuFeS_2). Main sulphides are pyrite, chalcopyrite and sphalerite. Main gangue minerals are quartz, feldspar, plagioclase and mica [11].



Figure 1: Circle shows the location of the Aitik tailing dam in Sweden (left) and the sampling place in the dam (right). (Google map, 2014).

Disturbed samples were taken from a depth of 0 to 0.7 meters in a trial pit. The trial pit was located at coordinates $67^{\circ}04'34''\text{N}$ and $20^{\circ}52'39''\text{W}$ (Figure 1, right) in the north east part of the dam. The sample from the trial pit was split into four different test specimens based on the size range by sieving (Table 1). Wet sieving was used with Sodium Diphosphate decahydrate ($\text{Na}_4\text{P}_2\text{O}_7 \cdot \text{H}_2\text{O}$) as a dispersant to enhance the particle separation. After sieving specimens were dried for 24 hours at 105°C . Remolded samples in 50mm diameter and 170mm length sampling tubes were casted by using the methodology describes by Dorby [12]. Dorby's procedure includes the filling of the tube specimen by steps, usually 5 to 6 in total, where each step comprises 2-3cm of the tube height. Water is added until the step is reached followed by the addition of the tailings sample and

posterior self-settlement for at least 6 hours. Same procedure is followed for every step until the tube is filled up. This methodology imitates the natural sedimentation process leading the tailings settle in beds with natural segregation. Since the test specimens are uniformly graded the segregation should be based on the grain density differences and not in the particle size. Basic geotechnical properties were determined for each sampling tube such as particle density, bulk density; saturated density, void ratio and degree of saturation (see Table 3).

Table 1: Test specimens and size ranges.

Specimen	Range (mm)
A	1-0.5
B	0.5-0.25
C	0.25-0.125
D	0.125-0.063

In order to study breakage due to increased vertical load the standard oedometer test (ASTM D 2435 -Method A) doubling the weight every 24 hours starting with 10, 20, 40, 80, 160, 320 and 640kPa load step under saturated and drained conditions was performed.

The oedometer sample dimensions are 20mm high and 40mm in diameter obtained from the remolded sampling tubes. Upper and lower parts of the oedometer were cover with end filters. The test specimens were mounted into the oedometer test rigged and submerged into water. The settlements were monitored by LVDT and the effect on the tailings particles was analyzed after the final load step. The generated amount of fines was determined by loss of mass after re-sieving the material after testing using the sieve for each test specimen respectively. Mass lost was used as measure on decomposition. An initial-state sample from each sample tube, A, B, C and D was collected and analyzed separately as basis for effects on shape change.

The effects on the individual tailings particles were studied by two-dimensional image acquisition followed by image analysis where changes in shape properties were studied.

As preparation for image acquisition the specimens were dried for 24 hours at 105° Celsius. The image acquisition was performed through a microscope (Motic B1) lightening sources from below and from the side of sample. The magnification lenses 4x was used for sample A and B and 10x for samples C and D. The magnification used for each sample was chosen based on the results obtained by Rodriguez et al. [13] where it was concluded that the minimum amount of pixels

that a particle should comprise is around 1800 pixels to minimize analysis errors. The camera mounted on top of the microscope (Infinity 2) has 2 megapixel resolutions. A more detailed description of the image acquisition process is described in Rodriguez et al. [13].

Table 2: Quantities use to determine the particle shape.

Quantity	Description	Reference
1	$4\pi\text{Area}/\text{Perimeter}^2$	[14]
2	$4\text{Area}/\pi\text{Major axis}^2$	[15]
3	Area/Convex Area	[16]
4	Fractal dimension	[17]
5	Square root of Maximum inscribed/Minimum circumscribed, circle diameters	[18]
6	Diameter of a circle same area as particle/Minimum circumscribed circle diameter	[19]
7	$\text{Perimeter}^2/\text{Area}^*$	[20]
8	Perimeter of a circle with same area/Perimeter	[19]
9	Area/Area of the minimum circumscribed circle	[21]
10	Perimeter/Convex perimeter *	[22]
11	$\text{Perimeter}/\pi\text{Average Feret}^*$	[23]

*Inverse was used to obtain a working range between 0 and 1

The 11 quantities in the Table 2 were used to determine the shape of the particles; graphical descriptions of the quantities are presented in the appendix. The two dimensional image analyses to determine the shape quantity was done by two different software; Image Pro Plus [17] and ImageJ [15].

Additionally as a control natural geological sand was tested in similar conditions to compare only the breakage and the shape change. This natural sand was obtained from a local sand extraction located 1 km north-west of the Luleå airport belonging to BDX industry AB (Sweden).

3 Results

Table 3 summarizes the basic properties of the tailings specimens before and after the oedometer test. Similar test were performed to natural sands, the basic properties for sand are in Table 4.

Table 3: Basic tailing properties.

Specimens tailings	Particle density (g/cm^3)	Void ratio (e)	Δe	Porosity n (%)	Δn (%)	Dry Density, ρ (gr/cm^3)	$\Delta \rho$
A	Initial	2.881	1.070	51.7	6.0	1.392	0.171
	Final		0.843	45.7		1.563	
B	Initial	2.904	0.849	45.9	4.4	1.571	0.129

	Final		0.708		41.5		1.700	
C	Initial		0.762		43.3		1.630	
	Final	2.873	0.669	0.093	40.1	3.2	1.722	0.092
D	Initial		0.847		45.9		1.589	
	Final	2.943	0.734	0.113	42.3	3.6	1.697	0.108

A number of 170 particles from each test specimens, before and after the oedometer test were analyzed for each shape quantity in Table 2. Basic statistical measures such as the mean, standard deviation and distribution curves were determined. A statistical t-test on 5 % significance level was tested for each shape quantity before and after the oedometer-test for each test specimen.

Table 4: Basic sand properties.

Specimens sand		Particle density (g/cm ³)	Void ratio (<i>e</i>)	Δe	Porosity <i>n</i> (%)	Δn (%)	Dry Density, ρ (gr/cm ³)	$\Delta \rho$
A	Initial	2.656	0.700	0,148	41.2	5.7	1.563	0.149
	Final		0.552		35.5		1.712	
B	Initial	2.651	0.740	0,118	42.5	4.2	1.524	0.111
	Final		0.622		38.3		1.635	
C	Initial	2.673	0.751	0,096	42.9	3.3	1.527	0.088
	Final		0.655		39.6		1.615	
D	Initial	2.684	0.954	0,156	48.8	4.4	1.374	0.119
	Final		0.798		44.4		1.493	

The distribution curves for quantities present a slightly skewed distribution and in approximately half of the quantities the distribution does not comply with the normality test for normal distributions. Normal distribution was achieved using Johnson transformation [24] but no differences in the results were observed thus, it was decided to continue without transform the data. In Table 5 the results are summarized. Bold-gray highlighted paired numbers represent those values where the mean of both populations (before and after test) show that they are different. Control specimens (natural sand) have shown no shape change (see Table 6). All changes in shape indicate that particles become more rounded except in Table 6 where “ \downarrow ” indicates that particles became more angular.

Table 5: Mean quantity values for tailing samples. Highlighted marked results show statistically significant changes in the shape quantities.

Sample	Quantity	Quantity										
		1	2	3	4	5	6	7	8	9	10	11
A	Before	0.665	0.753	0.9303	1.0339	0.6451	0.8011	0.1534	0.8458	0.6449	0.9197	0.2930
	After	0.660	0.742	0.9269	1.0339	0.6368	0.7918	0.1631	0.8484	0.6302	0.9290	0.2960
B	Before	0.690	0.735	0.9275	1.0414	0.6375	0.7945	0.0840	0.8626	0.6361	0.9405	0.2998
	After	0.712	0.746	0.9315	1.0390	0.6515	0.8049	0.0815	0.8804	0.6518	0.9530	0.3039
C	Before	0.702	0.713	0.9406	1.0292	0.6292	0.7853	0.0433	0.8795	0.6224	0.9599	0.3060
	After	0.695	0.744	0.9363	1.0286	0.6478	0.8035	0.0474	0.8770	0.6492	0.9513	0.3032
D	Before	0.694	0.693	0.9329	1.0492	0.6098	0.7759	0.0251	0.8729	0.6083	0.9603	0.3065
	After	0.722	0.738	0.9413	1.0439	0.6460	0.7973	0.0266	0.8919	0.6395	0.9638	0.3076

The degradation of the specimen was measured by quantifying the presence of finer material after oedometer-test. The amount of generated fines (in weight), determined by sieving, is presented in Table 7. Fines generated in tailings are higher in sample C but lower in A.

Table 6: Mean quantity values for the control sample, Natural sand

Sample	Quantity	Quantity										
		1	2	3	4	5	6	7	8	9	10	11
A	Before	0.730	0.705	0.952	1.022	0.637	0.789	0.135	0.890	0.628	0.966	0.307
	After	0.735	0.732	0.954	1.016	0.657	0.801	0.186	0.895	0.645	0.966	0.307
B	Before	0.736	0.723	0.948	1.034	0.643	0.794	0.081	0.895	0.634	0.969	0.309
	After	0.743	0.735	0.951	1.030	0.651	0.800	0.085	0.898	0.644	0.968	0.309
C	Before	0.742	0.731	0.954	1.023	0.653	0.815	0.047	0.031	0.698	0.970	0.309
	After	0.734	0.736	0.953	1.022	0.656	0.804	0.051	0.033	0.650	0.967	0.308
D	Before	0.744	0.717	0.951	1.040	0.643	0.793	0.027	0.903	0.633	0.974	0.311
	After	0.736	0.701	0.949	1.039	0.632	0.791	0.028	0.899	0.630	0.972	0.310

Table 7: The amount fines generated in the test specimens after the oedometer test

Specimen tailings	% fine content	Control specimen natural sand	% fine content
A	14	A	19
B	10	B	11
C	12	C	4
D	<1	D	2

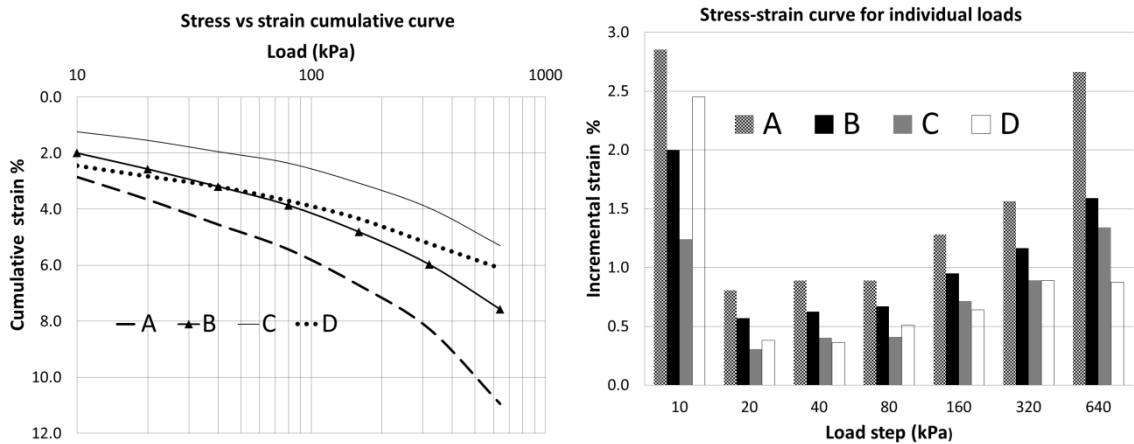


Figure 2: Semi-logarithmic stress-strain curve (left) and stress-strain bar by load step (right) from the oedometer test for the four tailings specimens.

Figure 2 (left) shows the stress-strain behavior where specimens A and B are weaker. Figure 2 (right) show that all specimens have initially high deformation, probably a result of initial rearrangement of the loose structures and re-distribution of stresses in the test specimens. The step strain for the test specimens A, B, and C differs from the specimen D behavior (Figure 2, right) because specimen D shows a high initial deformation and no significant difference in deformation between the two last load steps.

In s Figure 3 tress-strain curves of the tailings and control sand are plotted together. Dark lines represent the tailings while light lines are the control sands. It is interesting to see how the crossing of the lines of each size (sand-tailings) moves to the right for samples A, B and C but not for D. should D sample cross in higher stresses?. For coarse samples A and B there are more settlements for

tailings compare with sands.

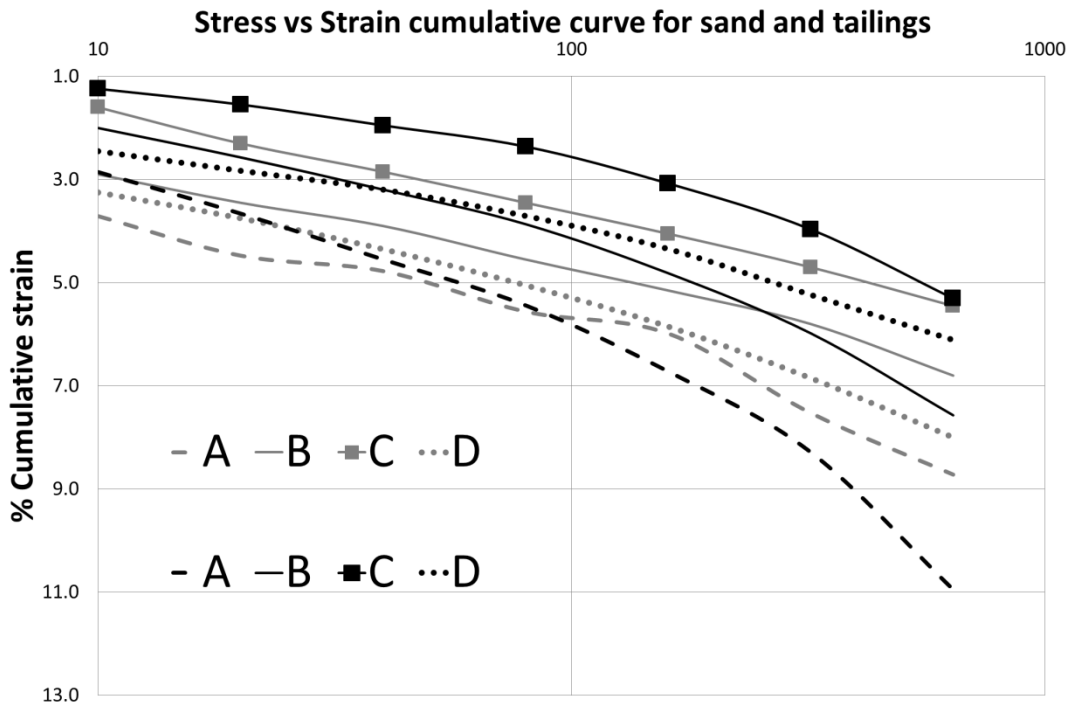


Figure 3: Stress-strain cumulative curve for sand and tailing samples. Dark lines represent tailings while light lines are the sands

4 Discussion

A disturbed sample of tailings was split by sieving into four, uniformly graded, test specimens and the effect on the uniformly graded test specimens upon vertical loading in an oedometer-test was compared.

The properties of the four tailings specimens are different. The coarsest tailing material sample 0.5mm, (A), is arranged in a looser state during the test specimen preparation and also showed the weakest stress-strain response in both, cumulative and step load (Figure 2, right). The analysis of the remaining material after the oedometer test showed that this test specimen also showed the highest degree of degradation measured as the generation of finer particles compared to the initial distribution (Table 7). The stress-strain behavior of the tailings specimens 0.125 (C) and 0.063 mm (D) are stiffer compared to the coarser 0.5 (A) and 0.25mm (B)

(Figure 2, left). Considering the degradation of the particles there is a big difference between specimen size 0.063mm and the others. The range of degradation is similar in specimen 0.5, 0.25 and 0.125 but is by methodology used in this study very low in specimen 0.063 mm. As Lade et al. [25] explained breakage increases while particle size increases due to the fact that larger particles contain more defects (or the probability to have it is higher) and depend also in the number of contacts per particle [7] in agreement whit Table 7 results.

Considering the shape factor tailings specimen D shows a statistical significant change in 8 of 11 quantities, considerable more than the rest (Table 5). In the specimen D (the finest fraction 0.063mm) shape change was observed in the majority of the shape quantities. This sample was also the most resistant to degradation, less than 1% of finer material was generated. According with the results it can be suggest that tailings sample D, due to the low % breakage (Table 7) and the quantity value change (Table 5) before and after the oedometer tests, is breaking only in the angularities or corners. Quantities 10 and 11 can also suggest this due to quantity 10 look for the concave outline change and since there is no difference it means that only corners are breaking while quantity 11 follows the same logic but in measuring two parallel line distances (feret box). In the finest fraction also a peculiar step load behavior, compared with the rest of the specimens, can be seen (Figure 2, right). Even if all the samples show an initial high compressibility the finest test sample D(0.063mm) seems to not be according with the rest of the stepped behavior of the samples A, B and C (major to minor in the initial load). Furthermore the two last load steps show no increase of percentage strain while the rest of the samples do. It shows a high initial compressibility but low at final loads.

By comparing the control specimens (natural sands) and tailing specimens it was observed that there was no general shape change in the control material maybe, because the particles already had been rounded by the time and natural elements through the years and they have lose their angularities. Even if there is a percentage in breakage in the control material there is no statistical evidence that the shape in average have change, maybe the new angular particles when generated due the breakage are no longer belonging to the specific size range and they were lost through the sieving (change of size). Stress-strain comparison of sands and tailings (Figure 3) suggest bigger settlements in tailings comparing by size for coarse samples A and B. it is interesting to see how tailings-sand lines (by size) start crossing to the right (for samples A, B and probably C) because the higher void ratios in tailings.

Breakage tailings-sands comparison by size in samples A and C seem to be different; for Sample A for sand and C for tailings looks higher. The high breakage of sand sample A could be due to angularities in the tailings brake (generating new angularities) and fines materials generate a stronger skeleton while sand break through the body reducing the size of the particles. Void ratio reduction also support this explanation been almost the double for tailings compared with sands. Sample C is believed that not only angularities break but the body as well explaining the higher fines generation. In this case the void ratio change is similar showing that even with the angularities tailing sample was relatively in the same initial packing state as sand sample was breaking the corners first and the body later.

This study shows that the degradation driven by increased vertical stress of tailings particles is different for different grain sizes under the same vertical loads. Coarser tailings are more susceptible compared to finer tailings. Coarse tailings are usually considered from a dam construction perspective to be more favorable since consolidation settlements are more rapid and hydraulic conductivity is higher. Cyclone techniques are sometimes applied to increase the coarser fraction at the beaches as a preoperational step for raising the tailings dams. The results from this study also indicate that there is a higher settlement as a result of particle degradation compared to the finer fractions.

5 Conclusions

Only fraction 0.063mm tailing particles show a shape change due to the corners becomes more rounded.

Coarse particles fraction 0.5mm present more breakage than the rest of the samples.

Coarse sample fractions 0.5 and 0.25mm produce higher settlements compare with the finer fractions and also compared with sands (by size).

Initial porosity seems to be the major factor affecting settlements.

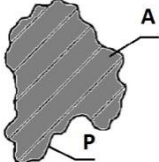
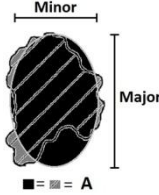
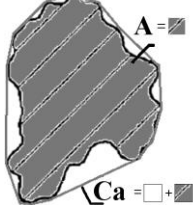
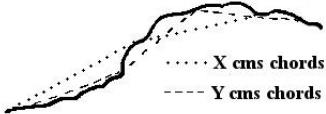
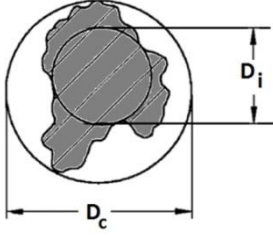
References

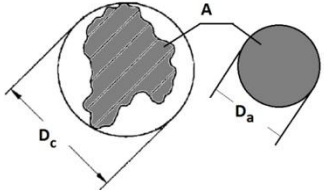
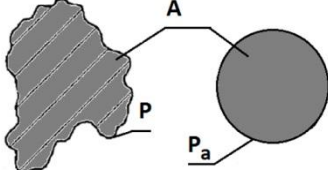
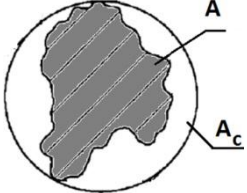
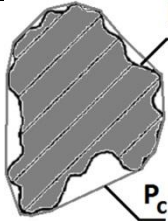
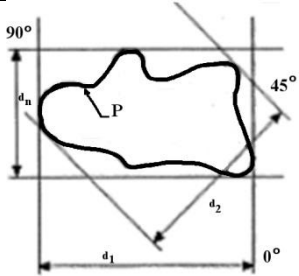
- [1] Ormann, Linda.; Zardai, Muhammad Auchar.; Mattson, Hans.; Bjelkevik, Annika and Knutsson, Sven. Numerical analysis of strengthening by rockfill embankments on an upstream tailings dam. *Canadian Geotechnical Journal*, **50**, (2013), pp. 391-399.

- [2] FHA. *User Guidelines for Waste and Byproduct Materials in Pavement Construction*. Department of Transportation, Federal Highway Administration, Washington D.C. USA, (1997).
- [3] Rodriguez J. and Edeskär T. Case of Study on particle Shape and Friction Angle on Tailings. *Journal of Advanced Science and Engineering Research*,**3**(4),(2013), pp. 373-387.
- [4] Garga, Vinod. K.; ASCE, M. and McKay, Larry. D. Cyclic Triaxial Strength of Mine Tailings. *Journal of Geotechnical Engineering*, **110**(8), (1984) pp.1091-1105.
- [5] Vick, S.G. *Planning, design and analysis of tailing dams*. Richmond, BC: BiTech Publishers Ltd.(1990).
- [6] Harding, Bobby. O. Crushing of soil particles. *Journal of Geotechnical Engineering*, **111**(10), (1985), pp. 1177-1192.
- [7] Valdes, Julio. R. and Koprulu, Eren. Characterization of fines produced by sand crushing. *Journal of Geotechnical and Geoenvironmental Engineering*, **113**(12),(2007), pp.1626-1630.
- [8] Fukumoto, Takeaki. Particle breakage characteristics of granular soil. *Soil and foundations*, **32**(1), (1992), pp.26-40.
- [9] Holubec and D’Apolonia. Effect of particle shape on the engineering properties of granular soils. *ASTM STP*, **523**, (1973), pp. 304-318.
- [10] Cho, G.; Dodds, J. and Santamarina, J.C. Particle shape effects on packing density, stiffness and strength: Natural and crushed sands. *Journal of Geotechnical and Geoenvironmental Engineering*, **132**(5), (2006), pp.591-602.
- [11] Lindvall, M. and Eriksson, N. Investigation of the weathering properties of tailings sand from Boliden’s Aitik copper mine – a summary of twelve years of investigations. *Proceedings 6th International Conference on Acid Rock Drainage*. Cairns, (2003).
- [12] Dorby, R. Soil properties and earthquake ground response. *Proceedings of the 10th European Conference on Soil Mechanics and Foundation Engineering*,**4**,(1991), Florence, Italy.
- [13] Rodriguez, J. M.; Johansson, J. M. A. and Edeskär, T. Particle shape determination by two-dimensional image analysis in geotechnical engineering. *Danish Geotechnical society bulletin*, **27**,(2012), pp. 207-218.
- [14] Cox, E. P. A method of assigning numerical and percentage values to the degree of roundness of sand grains. *Journal of Paleontology*, **1**(3), (1927), pp.179-183.

- [15] Ferreira and Rasband. *ImageJ user guide*,(2012), <http://imagej.nih.gov/ij/>
- [16] Mora, C. F. and Kwan, A. K. H. Sphericity, shape factor, and convexity measurement of coarse aggregate for concrete using digital image processing. *Cement and Concrete Research*, **30**, (3), (2000), pp.351-358.
- [17] Image Pro Plus v. 7.0. (2011). <http://www.mediacy.com/>.
- [18] Riley N. Allen. Projection Sphericity. *Journal of Sedimentary Petrology*, **11**, (2),(1941), pp. 94-97.
- [19] Wadell, H. Volume, shape, and roundness of quartz particles. *Journal of Geology*, **43**, (1935), pp.250-279.
- [20] Blott, S.J. and Pye, K. Particle shape: a review and new methods of characterization and classification. *Sedimentology*, **55**, (2008), pp.31-63.
- [21] Tickell, F. G. Effect of the angularity of grain on porosity and permeability. *Bulletin of the American Association of Petroleum Geologist*, **22**, (1938), pp.1272-1274.
- [22] Janoo, Vincent C. *Quantification of shape, angularity, and surface texture of base course materials*. Special report 98-1,US Army Corps of Engineers, Cold Region Research and Engineering Laboratory, (1998).
- [23] Kuo, C.-Y., Rollings, R., & Lynch, L. N. Morphological study of coarse aggregates using image analysis. *Journal of Materials in Civil Engineering*, vol. **10**, (3), (1998), pp.135-142.
- [24] Johnson, N. L. System of frequency curves generated by methods of translation. *Biometrika*, **36**(1/2), (1949), pp.149-176.
- [25] Lade, Poul. V.; Yamamuro, Jerry. A. and Bopp, Paul. A. Significance of particle crushing in granular materials. *Journal of Geotechnical Engineering*, **122**(4), (1996), pp. 309-316.
- [26] Johansson, Jens and Vall, Jakob. Friktionsjords kornform: Inverkan på geotekniska egenskaper, beskrivande storheter och bestämningsmetoder. Examensarbete. Luleå tekniska universitet, (2011), (in Swedish).

APPENDIX

Quantity	Description	Graphic description
1*	$4\pi \text{Area}(A) / \text{Perimeter}^2(P)$	
2*	$4 \text{Area}(A) / \pi \text{Major axis}^2(\text{Major})$	
3*	$\text{Area}(A) / \text{Convex Area}(Ca)$	
4	<p>Fractal dimension</p> <p>Fractal dimension use 'strides' (minimum step lengths) of various sizes. The fractal dimension is calculated as 1 minus the slope of the regression line obtained when plotting the log of the perimeter (for various strides) against the log of the stride length. (more info in imageproplus)</p>	
5*	<p>Square root of Maximum inscribed (D_i)/Minimum circumscribed (D_c), circle diameters</p>	

6*	Diameter of a circle same area as particle(D_a)/Minimum circumscribed circle diameter(D_c)	
7	$\text{Perimeter}^2(P)/\text{Area}(A)$	See figure in quantity 1 in this table
8*	Perimeter of a circle with same area (P_a)/Perimeter(P)	
9*	Area(A)/Area of the minimum circumscribed circle (A_c)	
10*	Perimeter/Convex perimeter	
11	$\pi \text{Average Ferret}/\text{Perimeter}(P)$ Average ferret box is obtained rotating two parallel lines (two degrees each time) and measuring the distance, finally the average ferret is the average distance of all the feret boxes distance measured	
* Figures were taken and modified from Johansson and Vall [26]		